INFN

Laboratori Nazionali di Frascati

LNF-88/08(R)
12 Febbraio 1988

C.Biscari, R.Boni, S.Kulinski, B.Spataro, F.Tazzioli, M.Vescovi:

AN INJECTOR FOR LISA

Servizio Documentazione
dei Laboratori Nazionali di Frascati
P.O. Box, 13 - 00044 Frascati (Italy)

INFN - Laboratori Nazionali di Frascati
Servizio Documentazione

LNF-88/08(R)
12 Febbraio 1988

AN INJECTOR FOR LISA

C.Biscari, R.Boni, S.Kulinski, B.Spataro, F.Tazzioli, M.Vescovi
INFN - Laboratori Nazionali di Frascati, P.O.Box 13, 00044 Frascati

1. - INTRODUCTION

The aims of the Project LISA (LInear Superconducting Accelerator) are explained in references 1 to 3, and may be summarized as follows:

1. building a superconducting linear accelerator with immediate application to a Free Electron Laser in the infrared .
2. implementing a test-bench machine for the construction of a larger accelerating system including superconducting linacs, recirculators and damping rings.

We will try to take into account the above considerations when designing the injection system for LISA.

2. - MAIN REQUIREMENTS FOR LISA INJECTION SYSTEM

The parameters of the LISA Injection System are mostly defined by:

- requirements of the electron beam for FEL;
- maximum input power limitations for the superconducting cavity unit.

The electron beam parameters required for the FEL of LISA are

-	Electron energy	$W \approx 30$ MeV
-	Energy dispersion	$\Delta W/W \leq 2.10^{-3}$
-	Peak current	$I_p = (5 \div 10)$A
-	Emittance (invariant)	$\varepsilon \leq \pi \cdot 10^{-5}$ m rad
-	Bunch length	$L_B \approx 3$ mm

Further we will see that except for the bunch length which must be shortened to below 1 mm all other parameters can be obtained by the proposed injection system.

Another important component of LISA which influenced the choice of the injection chain was the superconducting linac. The considerations which led to the choice of the superconducting structure - namely that proposed for HERA-DESY - are given in (1,4); here we will give only the most important parameters of the 4-cells section of this structure:

- Frequency — $F = 500$ MHz
- Quality factor (at T=4.2°k) — $Q = 2.10^9$
- Accelerating gradient — $E_{acc} = 5(7.5)$ MV/m
- Effective length for acceleration — $L_{eff} = 1.2$ m
- Energy increase — $\Delta W = 6\ (9)$ MeV
- Maximum (and average) power accepted by RF window — $P_{max} = 100$ kW

We begin our considerations by the power limitations of the superconducting section. Assuming that in principle the CW operation is not excluded we can calculate the maximum average current admissible by supposing that the whole input power is transferred to the beam. Taking a voltage increase $\Delta V = 7.5$ MV corresponding to an average value of the accelerating field $E_{acc} = 6.25$ MV/m, we obtain an average current I_{avm}:

$$I_{avm} = P_{max}/\Delta V_{max} = 100 \text{ kW}/7.5 \text{ MV} = 13.3 \text{ mA} \qquad (2.1)$$

This is the limit imposed by the maximum average power transmitted by the RF windows.

The peak current depends now on the type of operation. In the case of strictly CW operation with every RF micropulse filled with the charge bunch of duration T_B, the peak current I_p is given by:

$$I_p = I_{avm} \cdot T_{rf}/T_B \qquad (2.2)$$

where T_{rf} is the RF period of the accelerating field.

In the case when only every nth micropulse is filled with the charge of duration T_B, I_p can be obtained from the expression

$$I_p = I_{avm} \cdot T_{rf} \cdot n/T_B \qquad (2.3)$$

Assuming a bunch length $L_B \approx 3$ mm we have $T_B = L_B/\lambda_{rf} \cdot T_{rf} = 3/600 \cdot 2.10^{-9} = 10$ psec, and the phase length of the bunch $Df_B = L_B/l_{rf} \cdot 360° = 1.8°$.

Using Eq. (2.2) we obtain I_p:

$$I_p = I_{avm} \cdot T_{rf}/T_B = 13.3 \cdot 10^{-3} \cdot 200 = 2.66\text{A}$$

Then, to obtain e.g. I_p=10A, as required by the FEL operation, the bunch length must be about four times shorter, i.e. it should be equal to 0.8 mm corresponding to phase length of the bunch $\Delta\phi_B \approx 0.5°$.

In the case of filling only every nth RF microperiod the bunch length can be n times longer for the same average and peak currents. This kind of operation requires subharmonic chopper and prebuncher to be included in the injection chain (assuming that the "classical" thermo-cathode and not RF gun is used). Generally, the use of subharmonic chopper and prebuncher facilitates to obtain higher peak currents as it is seen from Eq. (2.3). It is then advisable to apply them especially in the systems in which high average currents and recirculations increasing these currents exist, as in the case of LISA.

It is obvious from the above examples that the obtainment of very short electron bunches with high current intensities requires rather complicated injection systems. These systems are common for FELs with high gain[5÷7] and also for larger facilities e.g. such as CEBAF[8]. Our injection chain, discussed below, will be similar to the above mentioned and especially to that of CEBAF.

3. - THE INJECTOR FOR LISA

To meet the requirements discussed above we propose to use the injector the general layout of which is presented in Fig. 1. The main parts of this system are:

- 100 keV gun
- compensated subharmonic chopper
- subharmonic prebuncher
- harmonic prebuncher
- 1 MeV harmonic capture section
- achromatic and isochronous transport line.

The other elements of the system are: solenoidal focusing lenses, steering coils and apertures to control the transport of the low energy electron beam into the first accelerating section. The RF elements of the injector up to and including the capture section are room-temperature components operating either at (250-500) MHz or at 3000 MHz (the second prebuncher and capture section). The 100-keV line produces an electron beam with a velocity of 0.55c, bunched into (0.5÷1.5) degrees bunches with energy dispersion of the order of 10% for injection into the capture section.

The harmonic capture section is an S-band graded β (β = 0.55÷0.94) standing wave structure giving at the output 1 MeV electron beam with about 1% energy dispersion and (1.5-6) degrees bunches. Taking into account that the ratio of frequencies between the capture section and the superconducting accelerator is 6, it would correspond to (0.25÷1.5) degrees

bunches at the input to SC sections, if the bunch length is conserved after the transport to the LINAC.

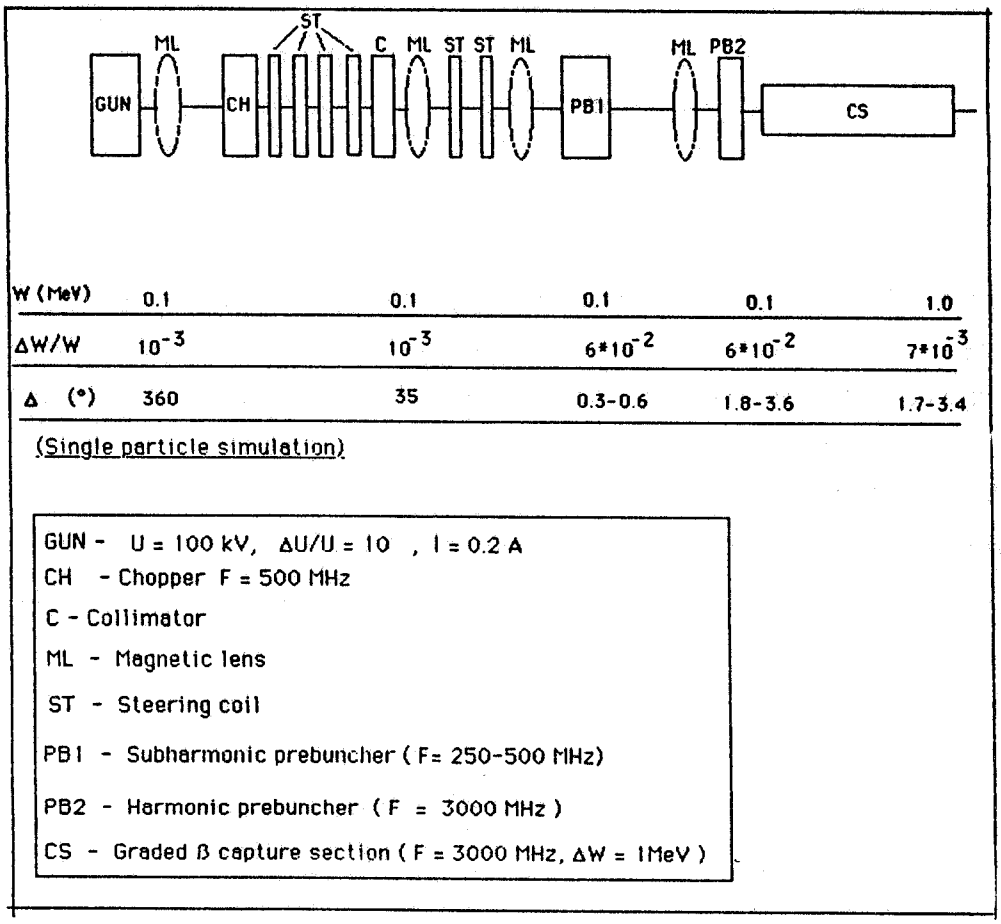

FIG. 1 - Sketch of LISA injector.

The electron beam coming out of SC sections will have average energy of 30 MeV with about 10^{-3} dispersion and (0.25÷1.0) degrees bunch length.

Schematically the changes of energy and bunch length along the injection chain are shown on Fig. 1.

Different programs were used to analyse and design the various components of the system. For the gun we used the SLAC Electron Optics program of Hermansfeldt modified by Sedlacek[9]. The RF components and particle dynamics were treated using a specially written program LISA[10], which analyses the axial motion without space charge, and PARMELA[11], which takes into account space charge, radial motion and finite emittance of the beam.

3.1. - The Gun

Required Parameters

Energy	$W_g = 100$ keV
Energy dispersion	$\Delta W_g/W_g = 10^{-4}(10^{-3})$
Emittance (invariant)	$\varepsilon \leq \pi \cdot 10^{-5}$ mrad
Current	$I = (0.1 \div 0.2)$A

The proposition is to use the Pierce geometry with grid (triode). In principle the operation is continuous but we would like to have the possibility of pulsed regime with pulse length of the order of 1 msec. That is why we propose the triode and not the diode even if the emittance of the triode could be a little worse than that of the diode.

The preliminary geometry of this gun found with the aid of SLAC Program is presented in Fig. 2, together with the beam envelope and equipotential lines[12].

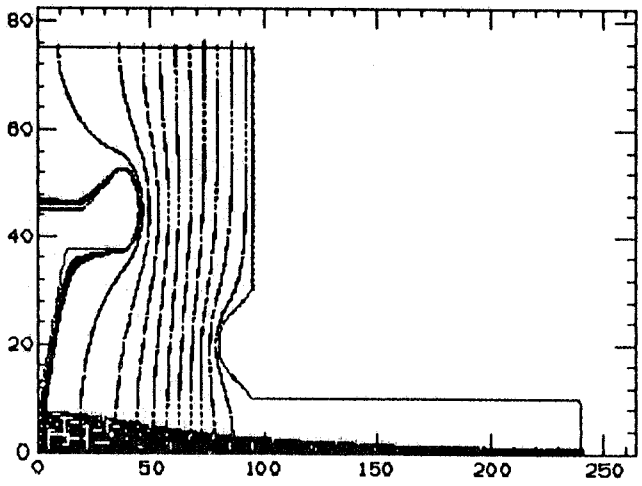

FIG. 2 - The geometry of the gun, electron trajectories and equipotential lines. U_a = 100 kV, U_{grid} = 445V; Beam current I = 0.7A; Beam emittance = 2.3 x 10^{-3} m rad. The waist of the beam with R_{min} =0.3mm is at about 90mm from the cathode.

Some other interesting parameters of this gun are:

- Cathode diameter $D_k = 6.4$ mm
- Current $I = 0.7$ A
- Emittance (invariant) $\varepsilon = 0.23 \cdot \pi \cdot 10^{-5}$ mrad

The waist of the beam with r_{min}=0.3mm is positioned at about 90mm from the cathode.

As it is seen from these data all the requirements concerning the gun can be satisfied by this proposition.

It is interesting to mention that at the beginning we considered the energy dispersion of the gun to be 10^{-4}. However, when analysing the bunching process we saw that the energy dispersion introduced by the prebunchers can be of the order of 10%; then it is not necessary to have such small energy dispersion of the gun and we decided that dispersion of the order of 10^{-3} will be

good enough, simplifing considerably the problem of the designe and construction of the power supply for the gun.

3.2. - RF Chopper

To obtain the high ratio between the peak current necessary for FEL and the average current accepted by SC structure because of power limitations, we should inject higher current intensity during only a part of a microwave period. This task is done by an RF chopper. In the case of LISA the bunch length transmitted by the chopper should be of the order of 30°-40° out of 360°. The chopper is a RF copper cavity at 500 MHz oscillating in the deflecting mode TE_{102} with a magnetic field B on the beam axis (see Fig. 3)

The trajectory of the deflected beam is shown in Fig. 4, where L is the length of the interaction region in the cavity, φ is the deflection angle, $\beta = v/c$ the relative speed of the electrons and $\gamma=W/W_0$. D is the length of the drift space before the collimator and s the transverse displacement at the collimator. The above quantities are related by the following formula:

$$B = 17.045\ \gamma\beta\ (\mathrm{tg}\ \phi/LT) \qquad (3.1)$$

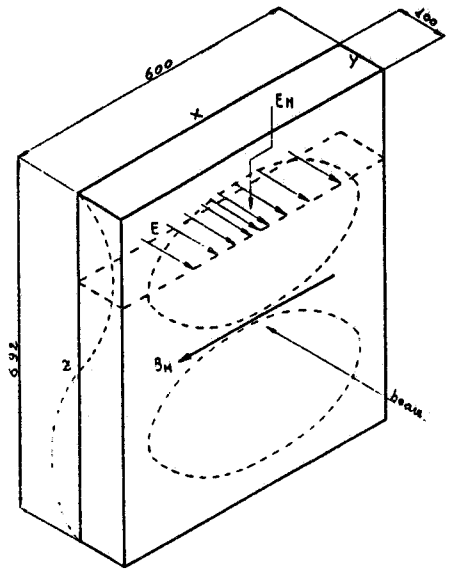

FIG. 3 - RF chopper cavity, mode TE102, f = 500MHz.

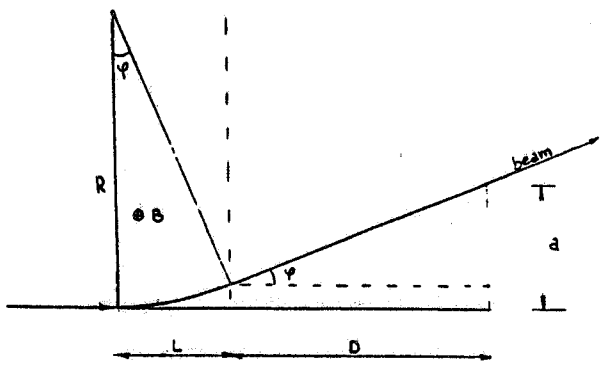

FIG. 4 - Trajectory of the deflected beam in the chopper.

with B in gauss, L in meters and $T=\sin(\pi L/\beta\lambda)/(\pi L/\beta\lambda) = 0.854$, transit time factor in the deflecting cavity.

The operation of the chopper in the biased mode is described below.

Fig. 5 shows a transverse section of the collimator hole, having radius r, and the beam spot

initially displaced by a quantity " a " by means of a D.C. magnetic field bias. Assuming that the diameters of the beam and the collimator are equal, the displacement of the beam follows the law:

$$s = a\,(1 - \sin\theta) \qquad (3.2)$$

with $\theta = wt$ and s the distance between the centers of the collimator and the beam. Referring to fig.5 and denoting by $\Delta\theta_0$ the chopping angle, i.e. the angle of the RF waveshape within which the beam current is transmitted, the following relation holds:

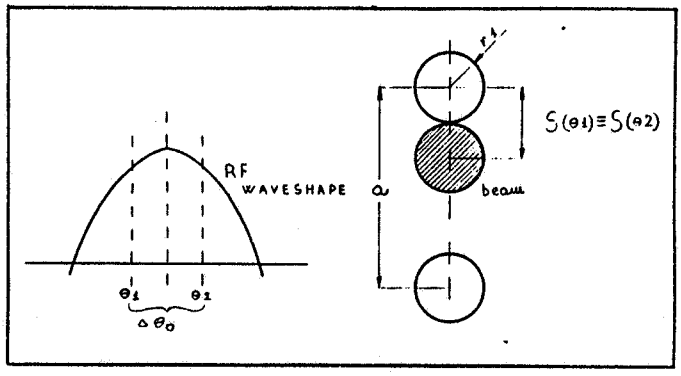

FIG. 5 - Chopping angle $\Delta\theta_0$ and the positioning beam-hole in the plane of the collimator.

$$r/a = [1 - \cos(\Delta\theta_0/2)\,] \qquad (3.3)$$

For : L = 0.1 m, D = 0.4 m, r = 1.5 mm, $\Delta\theta_0 = 35°$, it results:
a = 3.26 cm,
ϕ = 0.08 rad
B = 10.65 gauss.

The calculations made for the geometry of fig.3 give the results given below:

Xcm	Ycm	Zcm	Fo_{Mhz}	Q_o	P_d
60 cm	10 cm	69.2 cm	500	26000	755 W

3.3. - Prebunchers

The beam coming out of the chopper should be successively bunched in order to increase the peak current of the bunch and simultaneously to decrease the energy spread which depends on the bunch length in the following linear accelerators. Two prebunchers are proposed for LISA. The first one, having frequency either 250 MHz or 500 MHz, placed after the chopper and the other, harmonic buncher, placed directly before the capture section and oscillating at the same frequency of this section, F = 3000 MHz. Both prebunchers have similar structure. They are composed of klystron type microwave cavities working in the TM_{010} mode followed by corresponding drift spaces.

Two special subroutines were incorporated in the program LISA to design and analyse the effect of the prebuncher. Each of these subroutines at the beginning calculates the parameters of the prebuncher as a function of a bunching parameter BP given by

$$BP = \pi \cdot D \cdot V_{pB}/V_g \cdot \lambda \cdot \beta_g \qquad (3.4)$$

where

D	=	drift space
V_{pB}	=	prebuncher voltage
V_g	=	gun voltage
λ	=	wavelength of RF in prebuncher
$c \cdot \beta_g$	=	electron velocity corresponding to V_g.

Having found the parameters of the prebuncher the relativistic equation of axial motion is solved for a number of electrons with different phases forming the bunch. This procedure can be repeated for several values of the bunching parameter BP in order to optimize the bunch length and the energy dispersion at the end of the injection chain.

For the purpose of design we have assumed rectangular shape of the electric field in the gap of the prebuncher, but the numeric integration can be made with any realistic field distribution, e.g. of gaussian type or approximated by third order polynomials, measured experimentally field distribution.

Similar calculations were also performed with the aid of PARMELA in which it was necessary to make some modifications allowing for introducing the second prebuncher and a change of frequency in different elements. The problems connected with these modifications as well as others encountered when running PARMELA are discussed in the next chapters.

3.3.1. - The First Prebuncher PB1

Two frequencies were considered: 500 MHz and 250 MHz. The main parameters of these prebunchers are given below:

			F_{pB} = 500 MHz	F_{pB} = 250 MHz
- Prebuncher length	L_1	=	6 cm	12 cm
- Prebuncher Voltage	V_{pB1}	=	(10÷20)kV	(10÷20)kV
- Drift space (inversely proportional to V_{pB1})	D_1	=	(1.5÷0.75)m	(3÷1.5)m
- Bunching parameter	BP	=	1.35÷1.5	1.35÷1.5

It will be seen below that the best results were obtained for values of the bunching parameter BP1 ≈ (1.35÷1.50), corresponding to the case when in the curve: output-phase - $\varnothing_{out}$, input-phase - $\varnothing_{in}$ in there exist two points placed very closely to each other in which $d\varnothing_{out}/d\varnothing_{in} = 0$ (see Fig.6).

These two points denoted by B and C in Fig. 6 were also taken as a basis for calculation of the parameters of the second prebuncher PB2.

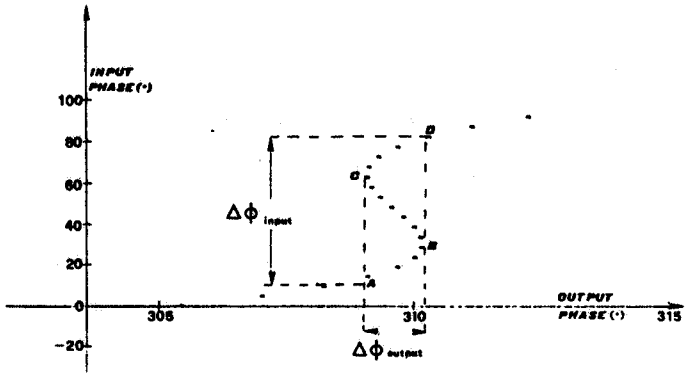

FIG. 6- A typical shape of the curve input phase-ϕ, output phase-fout of the first prebuncher in the case when the bunching parameter is close to the optimum.

3.3.2. - The Second Prebuncher PB2

Designing of the second prebuncher was a little more complicated. The idea of using it was as follows. We propose to use in the injection system an S-band 1 MeV capture section. It means that going from the output of PB1 to the input of the capture section all phases are multiplicated by the ratio of frequencies: F_{cap}/F_{pB1} which in our case can be 6 or 12. Then also the bunch length which at the output of PB1 is of the order of 1° corresponds to about 6 or 12 degrees at the input of the capture section. It seemed then useful to introduce the second prebuncher working at the same frequency as the capture section to compensate the effect of frequency change on the phase and to squeeze the length of the bunch before entering into the capture section. Looking at Fig. 6 it means that we should try to get closer all the points of the curve which lie between points A and D and especially those between B and C.

Taking into account that at the exit of PB1 the velocities of electrons corresponding to the points A, B, C, D of the curve in Fig. 6 fulfil the relation

$$v_{AO}<v_{BO}<v_{CO}<v_{DO}$$

then to get closer the points e.g. B and C at the exit of PB2 we should change the relation of velocities corresponding to these points and have

$$v_B>v_C$$

The designing of the prebuncher PB2 will consists then of:

1. Finding the proper entrance phase ϕ_0 of the bunch to PB2 (usually it will be the phase corresponding to the center of the bunch) in such a way as to accelerate the electrons being in the vicinity of points B and D and decelerate those in the vicinity of points A and C. The phase ϕ_0 should be optimized to minimize the voltage on PB2 necessary to obtain the desired relation between velocities v_B and v_C.

2. Finding the drift space D_2 which minimizes the bunch length.

The calculation of parameters for the second prebuncher is performed by a subroutine S-BUNCH (Second Buncher) of LISA. However, as the numerical results have shown, in our case the second prebuncher seems to be of limited application. It is due to the fact that the optimization of the parameters of the first prebuncher made in order to obtain very short bunch length at the exit of PB1 gives already for the phase difference $\Delta\phi_{BC}$ between the points B and C the value $\Delta\phi_{BC} \leq 0.5°$, so that the action of the second prebuncher has only a small effect. Nevertheless, taking into account that the dimensions of PB2 working in band S are small and that it can introduce some additional possibility of adjustment we propose to insert it in the injection scheme. Some preliminary parameters of the second prebuncher are given below.

-	Frequency	F_{pB2}	=	2998.5 MHz		
-	Length of prebuncher	L_{PB2}	≈	0.1 λ	=	0.01 m
-	Voltage	V_{PB2}	≈	17 kV		
-	Drift space	D_2	≈	0.096 m		

3.4. - Capture Section

Experience at the Darmstadt superconducting linac has shown that injection into a $\beta = 1$ superconducting capture section does not work well. Taking this into account, we propose after CEBAF solution to use a room-temperature capture section to increase the energy of the electrons to about 1 MeV before injection into a superconducting accelerator. In the case of CEBAF the frequency of the superconducting accelerator was 1500 MHz; it was natural to use the same frequency for the capture section. In our case the frequency of the cryogenic part is F_0=500 MHz; to avoid too large dimensions of the capture section we have decided to design an S-band capture section working at the sixth harmonic of the base frequency: F_{cs}= 2998.5 MHz. The main starting parameters for the design of this section are:

TYPE: STANDING WAVE, BIPERIODIC 1/2 π, GRADED β

-	Frequency	F_{cs}	=	2998.5 MHz
-	Input energy	W_{in}	=	0.1 MeV
-	Output energy	W	=	1 MeV
-	Length (approximate)	L	=	1 m

The cell lengths were calculated with the aid of the subroutine CELL of the Program LISA. The

above parameters were used as input data for this subroutine. Two assumptions were made:

1. Constant electric accelerating field along the structure;

2. Existence of the so called "synchronous" particle (particle which passes the centers of the accelerating cavities with the same phase relation to the RF field).

It means that the cell lengths must be chosen in such a way that the synchronous particle travels from the center of one accelerating cell to the center of the next one during the time equal to pT_{rf}. Here T_{rf} is the period of the RF accelerating field and p depends on the mode of accelerating field. E.g. p=1 for the mode 2π and p=1/2 for the mode π or for $\pi/2$ biperiodic structure. The results of the calculations are given in Table I. The capture section contains 26 cells (24 cells and two 1/2 cells at the extremities of the structure). The total length of the structure is 104 cm, β_0 = 0.54822, and β_{final} = 0.943037.

3.4.1. - Power Requirements

The power required for capture sections consists of two parts:

$$P_{cs} = P_B + P_{acc}$$

where

P_B = power delivered to the electron beam;
P_{Acc} = power necessary to produce the accelerating field in the cavity.

We assume here the continuous (CW) operation. We have then for P_B

$$P_B = I_{avm} * \Delta V = 0.013A * 0.9MV = 0.0117MW = 11.7kW$$

to calculate P_{Acc} we should know the shunt impedance of the structure. Now, for this kind of structure the effective shunt impedance ($Z_{sheff} = R_{sn} * T^2$, where T = transit time factor) changes between 42 and 63 MΩ/m for β = (0.55÷0.95) [13]. Taking the average value Z_{eff}=57.5 MΩ/m we obtain for P_{acc}.

$$P_{Acc} = V^2/Z_{eff} \cdot L = .81 * 10^{12}/57.5 \cdot 10^6 = 14.1 \text{ kW}$$

Then

$$P_{cs} \approx (11.7 + 14.1)kW = 25.8 \text{ kW} \quad (CW).$$

It is interesting to notice that similar results were also obtained for the $\pi/2$ standing wave

accelerating sections of the Mainz Microtron[14]: 15 kW/m of dissipated power and 15 kW of beam load. We also propose to use as RF power supply the same klystron TH 2075 which gives 50 kW of output power.

3.5. - Isochronous transport line

The geometry of LISA recirculators[15] constrains the injector system to be not on the same axis of the SC LINAC.

The transport line between the capture section and the SC LINAC should be achromatic to avoid dispersion in the horizontal phase plane and isochronous to avoid lengthening of the bunch.

Being electrons not ultrarelativistic at the injection energy (W_{in}=1.MeV, β_{rel}=0.94), the spread in time arrival due to the energy spread has been taken into account when designing the transport line and has been compensated by the spread in trajectory lengths introduced by the dispersion function.

The injector chain results parallel to the SC LINAC; the transport line consists of one quadrupole triplet wich matches the betatron functions of the exit of the capture section to the following arc and an arc of 180°; the arc contains three dipoles (45°,90° and 45° respectively), and two symmetric quadrupole doublets which adjust the dispersion function to the isochronism condition. A more detailed description of the line can be found in reference 16.

The layout of the transport line is depicted in Fig. 7. The characteristics of its elements are given in Table II. The optical functions are represented in Fig. 8.

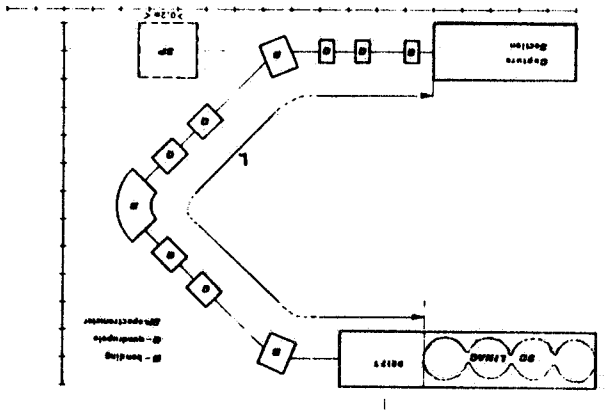

FIG.7- Sketch of the transport line between the injector and the SC linac.

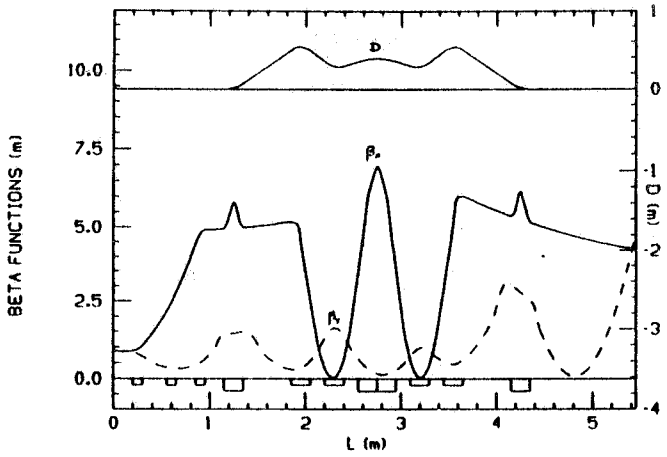

FIG. 8 - Optical functions in the transport line injector-SC linac.

4. - NUMERICAL SIMULATION

Having specified the elements of the injection system we should now optimize the parameters of the different parts of that chain in order to get the desired properties of the beam at the output of the superconducting linac. To perform this optimization it is necessary to calculate the behaviour of the beam along the whole injection chain for a set of parameters of the different elements of the system. Two programs were again used for these calculations: LISA and PARMELA.

4.1. - Optimization and Simulation with LISA

As it has been already mentioned LISA is a program which can either design the different elements of an injection system and/or calculate the axial dynamics (without space charge) of particles moving in such systems. For dynamic calculations the axial distribution of the electric field intensity can be approximated by the third order polynomial in axial variable allowing for high fidelity reproduction of the measured or calculated axial electric field distribution. Two parameters were optimized using LISA:

- The amplitude of the electric field intensity in the capture section. Assuming that the axial distribution of the electric field intensity is as that shown in Fig. 9, which is a typical

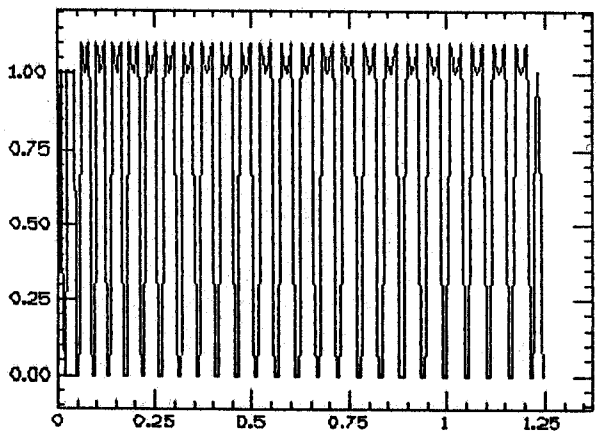

FIG. 9 - Axial electric field distribution along the capture section.

distribution for this kind of structures, the optimum value for the amplitude E_m was found to be E_m = 1.6 MV/m. It assures that electrons pass the centers of the accelerating cavities at times when the phases are close to 180° i.e. when the accelerating field is maximum. In PARMELA, which uses the average field and not the amplitude, it corresponds to E_0 = 1.1 MV/m.

- The bunching parameter of the first prebuncher PB1. The results of this optimization are given in Table III and are also shown in Figs. 10 and 11.

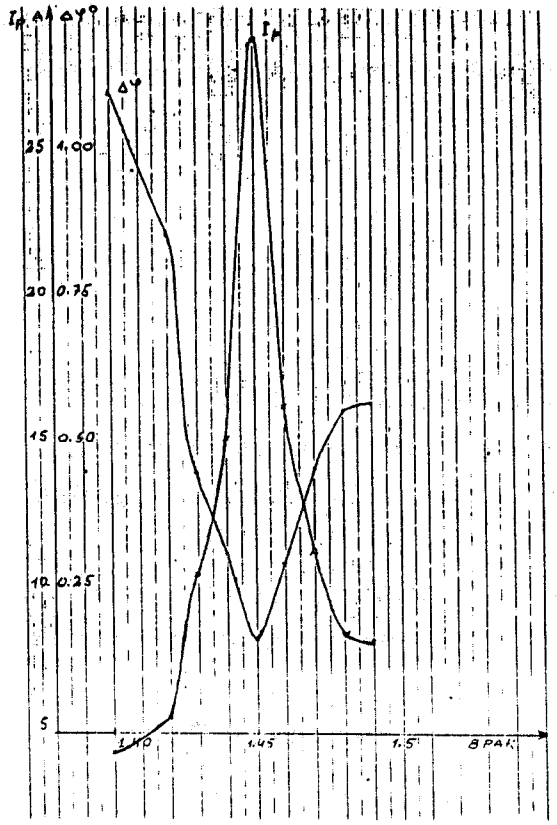

FIG. 10 - Changes of the peak current I_p and the bunch legth $\Delta\phi$ at the end of the capture section as a function of the bunching parameter B_{par} F_{PB1} = 500 MHz, V_{PB1} = 10 kV. Drift length = 1.43 m. No second prebuncher.

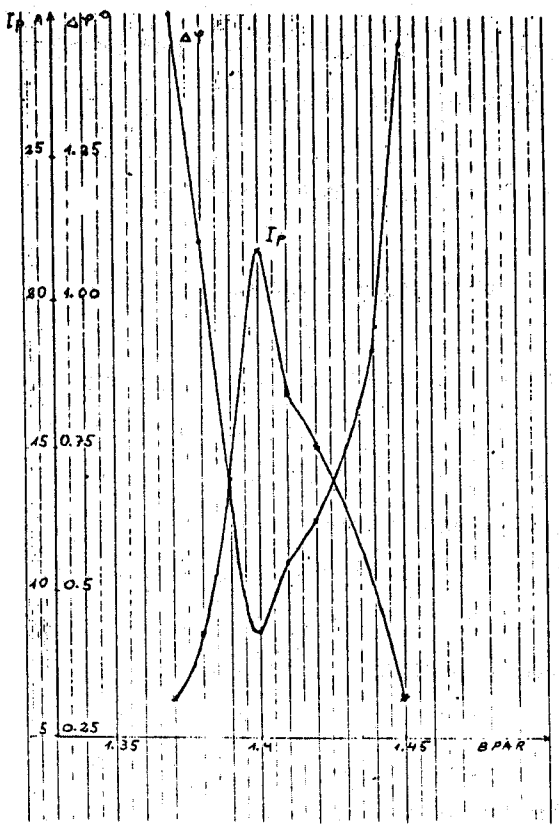

FIG. 11 - Change of the peak current I_p and the bunch length $\Delta\phi$ at he end of the capture section as a function of the bunching parameter B_{par} F_{PB1} = 250MHz, V_{PB1} = 20 kV. Drift length = 1.39m. No second prebuncher.

Two frequencies were considered: F_{PB1} = 500 MHz and 250 MHz. As it can be seen from Figs. 10 and 11 in both cases the peak currents have similar maximum values exceeding 20A. It may appear then that the case of F_{PB1}= 500 MHz could be prefered since e.g. it is easier to realize and the dimensions are twice smaller. However there exist at least two reasons for which it is interesting to continue the study also for F_{PB1}= 250 MHz:

1. We will see later that the longitudinal space charge effects are smaller in the case of F_{PB1}=250 MHz because of the longer bunch length, so that the effective maximum peak current can be higher for this frequency.

2. It seems also that there exists the possibility of constructing a gun whose electronics would allow very short current pulses with duration time 1nsec and repetition frequency in the range of (200 : 250) MHz. In that case there would be no need to use the chopper because such short pulses could be directly applied to the prebuncher if the gun repetition frequency is equal to that of the prebuncher.

Another thing which is clearly seen from Figs. 10 and 11 is that the peak current depends strongly on the bunching parameter BP, e.g. the change of BP by only 2% (which is equivalent to the same change of effective voltage on the prebuncher assuming the drift space constant)

increases twice the phase dispersion at the output of the capture section and decreases twice the peak current. It means that to obtain the high peak currents the voltage of the prebuncher must be regulated very smoothly (in steps smaller than 1%) and that the stabilization of this voltage must be better than 1%.

4.2. - Simulation with PARMELA

4.2.1 - Particle dynamics

Program PARMELA has been used to complete the single particle simulation described in the previous paragraph by a three dimensional calculation. The code performs the tracking of N particles along a transport line which must be completely defined, the program not performing any optimization of parameters.

Each particle is described by the 6 coordinates (x,x',y,y',z,W), generated in distributions which can be random or uniform in each phase plane or in superspaces of the 4 transverse dimensions or of the 6 dimensions.

In order to clarify the following results, we will spend some words on the definitions of the beam characteristics as seen by a PARMELA user.

The rms emittance of a set of particles in the (x,x') phase plane can be defined by[17]:

$$\varepsilon_{rms} = \sqrt{\langle x^2 \rangle \langle x'^2 \rangle - \langle x\, x' \rangle^2}$$

The value of the emittance, as usually intended (area of the phase plane), is related to ε_{rms} by a constant k^2 ($\varepsilon = k^2\, \varepsilon_{rms}$) whose value depends on the distribution function of the coordinates: if the distribution is uniform, $k^2 = 4$.

It is possible to define the equivalent of the Twiss parameters as

$$\alpha = -\langle xx' \rangle / \varepsilon_{rms} \qquad \beta = \langle x^2 \rangle / \varepsilon_{rms} \qquad \gamma = \langle x'^2 \rangle / \varepsilon_{rms}$$

The envelope of the distribution is then defined as

$$e = k \langle x^2 \rangle^{1/2}$$

The α, β above defined are not necessarely a periodic solution of a Twiss equation, but if tracked along a linear system they behave as the usual Twiss parameters, so that their value has been taken as starting point for the design of the transport line between the capture section and the Linac.

PARMELA has been completed with a subprogram which computes ε, α, β and e as stated

above, with graphic possibilities. To avoid that particles which are far from the edges of the bunch distort the results, the averages on the coordinates are taken on the 90% of the distribution.

The original version of the program allowed for only one fixed frequency during a run. We have modified the code in order to have the possibility of defining different frequencies along the line, in our case the frequencies of the subharmonic prebuncher, of the second prebuncher and finally of the SC linac.

The program performs also space charge calculations. The bunch is divided into rings of charge and the effects of all the rings on each particle are summed up. The influence of space charge impulses on the bunch behaviour is very much depending on the dimensions of the mesh used to subdivide the bunch into rings and up to now is not very clear to us which is the more fitting choice; while the mean transverse dimensions of the bunch are almost conserved along the line, the bunch length change by a large factor during the transport and the definition of the longitudinal mesh must be renewed during the calculations. So we dare say the results obtained must be interpreted just as an indication which is good so far the average current is not too high (in our case I_{avm} = 13 mA).

We will briefly describe the treatment of each element of the line.

- The focusing in the transverse plane is ensured by solenoidal lenses placed in the drifts along the line or solenoidal fields superimposed on the capture section. The first guess for the position and strength of the solenoids has been obtained with the help of the code BEAM[18], where gaussian shape of the magnetic field distribution is assumed. Field intensities of the order of some hundreds of gauss are sufficient to keep the beam envelope under 2mm from the chopper to the capture section. In PARMELA solenoids are simulated by rectangular distributions of the magnetic fields plus the effect of fringing fields.

- The prebuncher has been treated as a cavity with a purely sinusoidal time variation of the field on axis, e.g. the electric field represented in Fig. 9 has been approximated by a rectangular distribution. The synchronous phase at the gap center has been chosen so that the center of the bunch in phase corresponds to the particle with mean energy. The field intensity has been optimized in order to obtain at the end of the drift between the prebuncher and the capture section the shortest bunch length. When space charge is included in the simulation, the voltage in the prebuncher must be increased by 30 ~ 50% to take care of the defocusing effect of space charge in the longitudinal plane.

- The capture section has been designed with the program, assuming π-mode cells and a flat field distribution, choosing the field intensity and the design phase similar to those used in program LISA, but adjusting them slightly to take care of the different field distributions used. The possibility of adding a superimposed solenoidal field along the section has been introduced in the program.

- The SC LINAC has been simulated by two sections which represent the two criostats, each one consisting of two groups of 4 cells (π -mode), adjoined by drifts of $\beta\lambda$ length. In between the two criostats a drift of $\beta\lambda$ length has been introduced where a quadrupole doublet accounts for the transverse focusing. An accelerating gradient of 6MV/m has been assumed, giving a final energy of 30MeV.

4.2.2 - Results of the simulation

The simulation has been performed from the exit of the chopper cavity to the end of the capture section along the line with the 250 MHz prebuncher and the line with the 500 MHz prebuncher; the 2nd prebuncher is not considered in these simulations.

The transport to the SC LINAC, along the isochronous transport line and along the LINAC itself, has been performed only for the case of the 500MHz prebuncher.

The following input distribution of particles has been assumed:

- Random distribution in the horizontal phase plane with

$$\alpha_x = 0. \quad \beta_x = .23 \text{ m} \quad \varepsilon_x = 10^{-5} \text{ m rad}$$

- Random distribution in the vertical plane plane with

$$\alpha_y = 0. \quad \beta_y = .23 \text{ m} \quad \varepsilon_y = 10^{-5} \text{ m rad}$$

- Uniform distribution in the longitudinal phase plane with

$$\Delta\phi = 35^\circ \quad \Delta W/W = 0.$$

The effect of the chopping cavity both in transverse and in longitudinal phase planes has not been taken into account ($\alpha_x = \alpha_y = 0$); further investigations are needed on this point.

The results of the particle simulation are summarized in Table IV, which contains the characteristics of the bunch at the exit of the chopper, at the input of the capture section and at its exit for the lines with the prebuncher at 250MHz and at 500MHz. The results include space charge effects.

The results in absence of space charge are in good agreement with those of LISA described above.

The bunch which passes through the line with the prebuncher at 500MHz has been followed along the transport line and the SC LINAC. Its characteristics at the input of the SC accelerating cells and at the end of the LINAC are also given in Table IV.

The horizontal emittance ε_x grows along the transport line by a factor 1.5; the final value

after the acceleration to 30MeV is $\varepsilon_x=1.2*10^{-7}$ m rad, which fulfil the requirements of FEL operation.

The bunch lengthens along the transport from the capture section to the SC LINAC by 20%. This lengthening can be explained by the different trajectories particles follow due to the betatron oscillations in the magnets, which can reach amplitudes of 5mm. The final length of the bunch is 1mm, which corresponds to a peak current of $I_p=8A$, in agreement with the requirements of FEL operation.

Transverse envelopes, β functions and emittances from the chopper to the end of the capture section as obtained from PARMELA simulations are represented in Figs.12-14. Figs.a refer to the lines whith the 250-MHz subharmonic prebuncher, while Figs.b correspond to the line with the 500MHz prebuncher.

Figs. 15-17 give the same parameters from the capture section through the transport line to the end of the SC LINAC.

Figs. 18-20 represent the phase space plots for the complete line in the more interesting spots (on the plots of phase planes the 100% of particles are plotted, but the emittance ellips refers to the 90%).

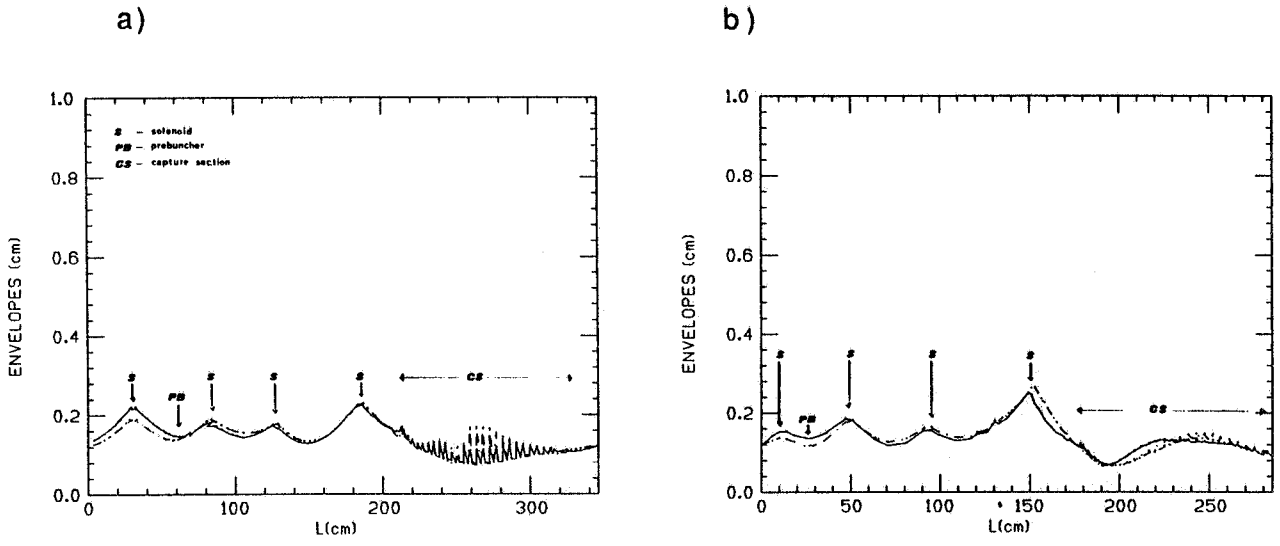

FIG.12 - Transverse envelopes along the injector: _____ Horizontal . _ . _ . _ Vertical.
a) Prebuncher at 250 MHz; b) Prebuncher at 500 MHz.

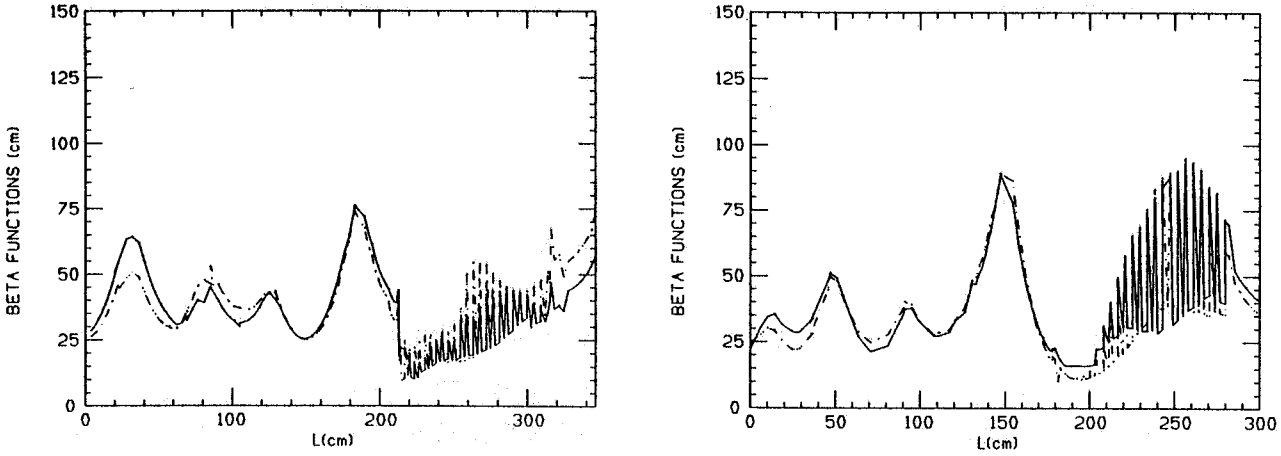

FIG. 13 - Beta functions along the injector. _____ Horizontal . _ . _ . _ Vertical.
a) Prebuncher at 250 MHz; b) Prebuncher at 500 MHz.

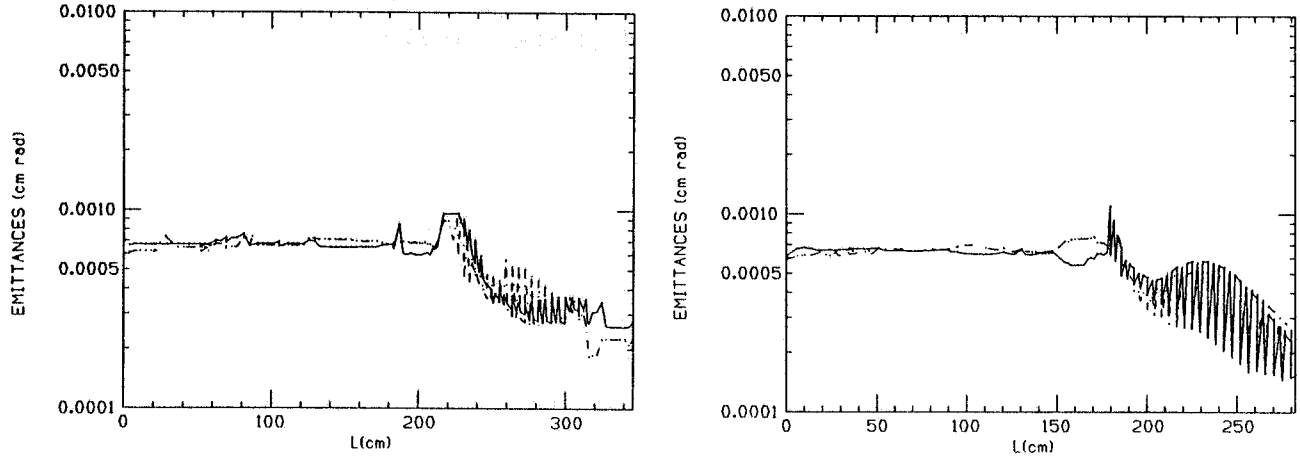

FIG.14 - Emittances along the injector:_____ Horizontal . _ . _ . _ Vertical.
a) Prebuncher at 250 MHz; b) Prebuncher at 500 MHz.

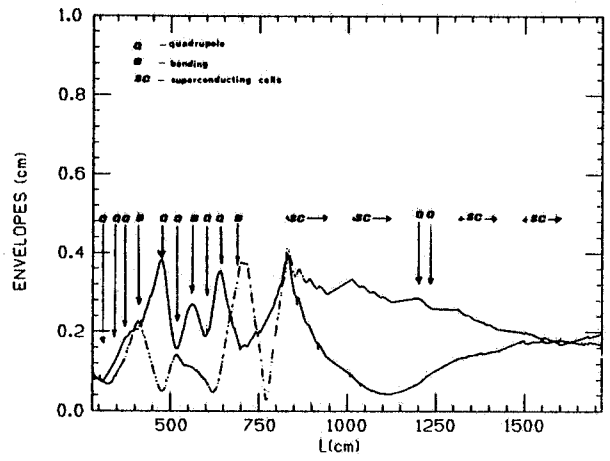

FIG.15 - Transverse envelopes along the transport line and the SC linac: _____ Horizontal _ . _ . _ Vertical Prebuncher at 500 MHz.

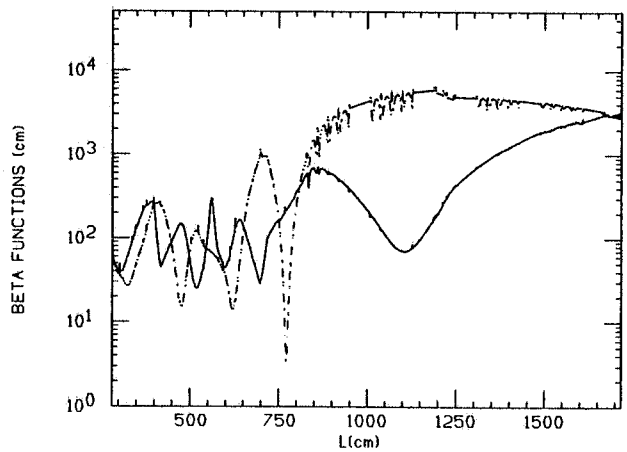

FIG.16 - Beta functions along the transport line and the SC linac: _____ Horizontal . _ . _ . _ . Vertical Prebuncher at 500 MHz.

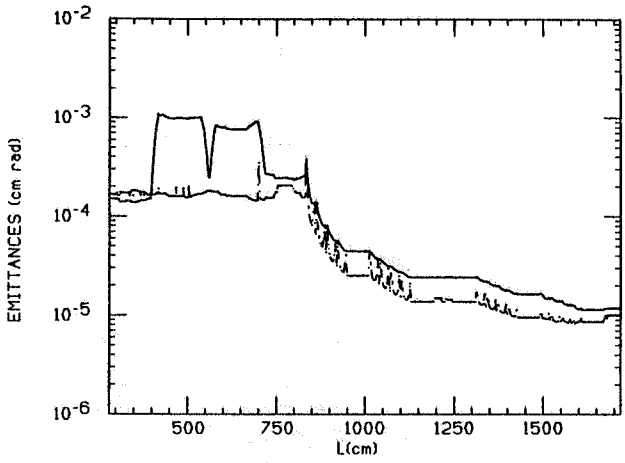

FIG.17 - Emittances along the transport line and the SC linac: _____ Horizontal ._._._ Vertical Prebuncher at 500 MHz.

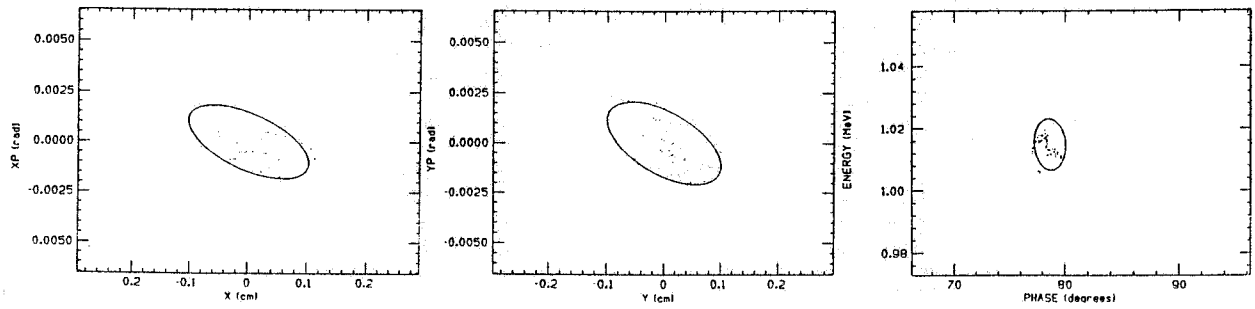

FIG.18 - Distribution of particles in the three phase planes at the input of the capture section.

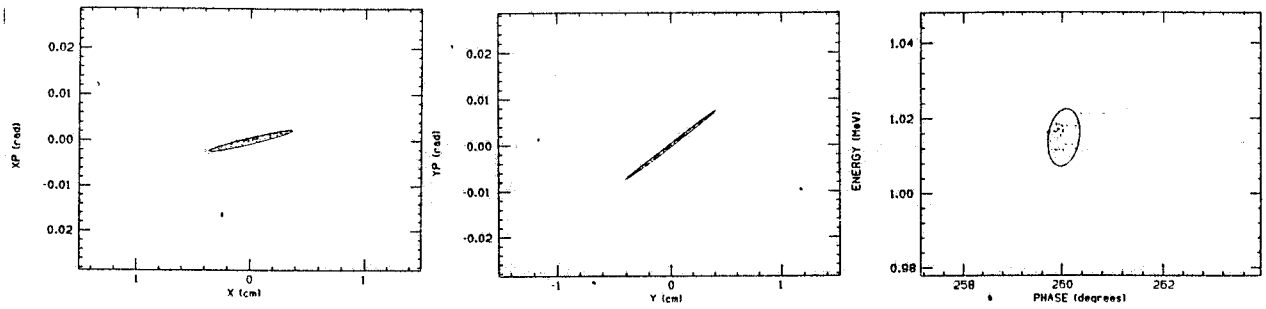

FIG. 19 - Distribution of particles in the three phase planes at the output of the capture section.

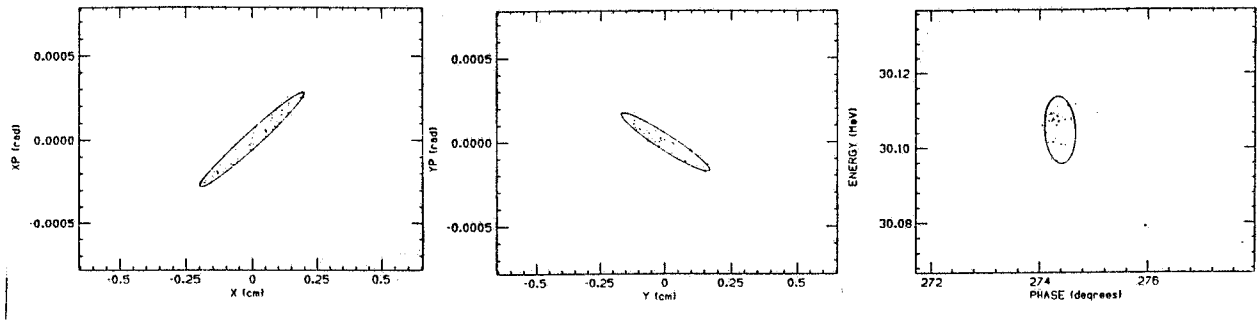

FIG. 20 - Distribution of particles in the three phase planes at the output of the SC linac.

TABLE I - Parameters of the graded β noramal conducting 1 MeV capture section.

NC	BETA	GAMMA	ENERGY (MeV)	CELL LENGTH (m)	LINAC LENGTH (m)
1	0.5845724E+00	0.1220383E+01	0.1126164E+00	0.1461151E-01	0.1461151E-01
2	0.5845724E+00	0.1272896E+01	0.1394511E+00	0.2922301E-01	0.4383452E-01
3	0.6391766E+00	0.1329172E+01	0.1682085E+00	0.3195270E-01	0.7578722E-01
4	0.6767192E+00	0.1388754E+01	0.1986550E+00	0.3382947E-01	0.1096167E+00
5	0.7096380E+00	0.1451234E+01	0.2305826E+00	0.3547509E-01	0.1450918E+00
6	0.7384867E+00	0.1516254E+01	0.2638081E+00	0.3691725E-01	0.1820090E+00
7	0.7637827E+00	0.1583502E+01	0.2981718E+00	0.3818181E-01	0.2201908E+00
8	0.7859917E+00	0.1652704E+01	0.3335346E+00	0.3929204E-01	0.2594829E+00
9	0.8055267E+00	0.1723627E+01	0.3697763E+00	0.4026860E-01	0.2997515E+00
10	0.8227463E+00	0.1796066E+01	0.4067928E+00	0.4112942E-01	0.3408809E+00
11	0.8379648E+00	0.1869844E+01	0.4444940E+00	0.4189020E-01	0.3827711E+00
12	0.8514515E+00	0.1944810E+01	0.4828020E+00	0.4256441E-01	0.4253355E+00
13	0.8634355E+00	0.2020832E+01	0.5216491E+00	0.4316349E-01	0.4684990E+00
14	0.8741210E+00	0.2097794E+01	0.5609770E+00	0.4369766E-01	0.5121967E+00
15	0.8836690E+00	0.2175596E+01	0.6007345E+00	0.4417497E-01	0.5563716E+00
16	0.8922315E+00	0.2254153E+01	0.6408772E+00	0.4460301E-01	0.6009746E+00
17	0.8999273E+00	0.2333387E+01	0.6813661E+00	0.4498773E-01	0.6459624E+00
18	0.9068650E+00	0.2413232E+01	0.7221673E+00	0.4533455E-01	0.6912969E+00
19	0.9131365E+00	0.2493629E+01	0.7632505E+00	0.4564806E-01	0.7369450E+00
20	0.9188178E+00	0.2574526E+01	0.8045894E+00	0.4593207E-01	0.7828770E+00
21	0.9239817E+00	0.2655878E+01	0.8461606E+00	0.4619022E-01	0.8290672E+00
22	0.9286854E+00	0.2737644E+01	0.8879434E+00	0.4642536E-01	0.8754926E+00
23	0.9329829E+00	0.2819789E+01	0.9299196E+00	0.4664019E-01	0.9221328E+00
24	0.9369121E+00	0.2902279E+01	0.9720725E+00	0.4683661E-01	0.9689694E+00
25	0.9405164E+00	0.2985087E+01	0.1014388E+01	0.4701679E-01	0.1015986E+01
26	0.9430373E+00	0.3026602E+01	0.1035602E+01	0.2357141E-01	0.1039558E+01

TABLE II - Elements of the isochronous transport line.

	ELEMENT	TYPE	LENGTH(m)	$K^{-2}(m^{-2})$
1	DRIFT		0.20	
2	QUAD		0.10	- 15.
3	DRIFT		0.25	
4	QUAD		0.10	- 2.
5	DRIFT		0.20	
6	QUAD		0.10	10.
7	DRIFT		0.20	
8	RBEND		0.20 (θ=45°)	
9	DRIFT		0.50	
10	QUAD		0.20	16.9140
11	DRIFT		0.15	
12	QUAD		0.20	- 21.4636
13	DRIFT		0.15	
14	SBEND		0.40 (θ=90°)	
15	DRIFT		0.15	
16	QUAD		0.20	- 21.4636
17	DRIFT		0.15	
18	QUAD		0.20	16.9140
19	DRIFT		0.50	
20	RBEND		0.20 (θ=45°)	
21	DRIFT		0.50	
22	DRIFT		0.60	

TABLE III - Phase and energy dispersion dependence the beam in the injector on the bunching parameter BP1. Simulation without space change.

First prebuncher PB1 Δφ = 40°					Capture section W_{in}=0.1MeV W_{out}=1MeV			
Freq (MHz)	Bunching parameter	V PB1 (kV)	$\Delta\phi_{out}$ (°)	$\Delta W/W_{out}$	$\Delta\phi_{in}$ (°)	$\Delta\phi_{out}$ (°)	$\Delta W/W_{out}$ ($\times 10^3$)	I_p (A)
250	1.37	20	0.43	0.11	5.2	8.8	6.9	6.8
250	1.38	20	0.23	0.11	2.7	6.4	8.0	9.6
250	1.39	20	0.27	0.11	3.2	4.0	9.3	16.1
250	1.40	20	0.40	0.11	5.0	2.6	12.0	23.3
250	1.41	20	0.60	0.11	7.3	3.3	13.0	15.3
250	1.42	20	0.80	0.11	9.8	3.8	15.0	13.8
250	1.45	20	1.40	0.11	17.3	8.7	22.0	6.9
250	1.50	20	1.70	0.11	20.5	17.8	20.0	5.1
500	1.40	10	1.30	0.06	8.0	6.4	3.8	4.7
500	1.42	10	1.10	0.06	6.6	5.1	4.4	7.2
500	1.43	10	0.60	0.06	3.7	2.7	5.5	11.9
500	1.44	10	0.39	0.06	2.3	1.9	4.9	18.1
500	1.45	10	0.28	0.06	1.7	1.0	6.0	24.3
500	1.46	10	0.30	0.06	1.8	1.7	6.6	14.8
500	1.47	10	0.47	0.06	2.8	2.4	7.8	10.6
500	1.48	10	0.61	0.06	3.7	3.3	8.6	8.4
500	1.49	10	0.70	0.06	4.2	3.4	6.7	8.2

TABLE IV - Bunch characteristics along the injector system.

	OUTPUT CHOPPER	INPUT CAPTURE SECTION	OUTPUT CAPTURE SECTION	INPUT SC CELLS	OUTPUT CRIOSTAT
F_{PB1} = 250 MHz					
α_x	0.0	-0.1	-0.02		
β_x(m)	0.23	0.4	0.5		
ϵ_x(m rad)	$6.\ 10^{-6}$	$6.6\ 10^{-6}$	$2.7\ 10^{-6}$		
$\gamma\beta\epsilon_x$(m rad)	$4.\ 10^{-6}$	$4.2\ 10^{-6}$	$7.5\ 10^{-6}$		
e_x(mm)	1.2	1.7	1.1		
α_y	0.0	-0.1	-0.2		
β_y(m)	0.23	0.4	0.7		
ϵ_y(m rad)	$6.\ 10^{-6}$	$7.0\ 10^{-6}$	$1.8\ 10^{-6}$		
$\gamma\beta\epsilon_y$(m rad	$4.\ 10^{-6}$	$4.4\ 10^{-6}$	$5.1\ 10^{-6}$		
e_y(mm)	1.2	1.6	1.1		
W_0(MeV)	0.100	0.094	1.005		
$\Delta W/W_0$	0.0	$8.8\ 10^{-2}$	$1.8\ 10^{-2}$		
$\Delta\phi°$	17.5	3.2	2.1		
e_l(mm)	16.0	0.5	0.6		
F_{PB1} = 500 MHz					
α_x	0.0	0.3	0.7	-3.3	-4.5
β_x(m)	0.23	0.22	0.7	5.4	33.
ϵ_x(m rad)	$6.\ 10^{-6}$	$6.7\ 10^{-6}$	$1.5\ 10^{-6}$	$2.5\ 10^{-6}$	$1.2\ 10^{-7}$
$\gamma\beta\epsilon_x$(m rad)	$4.\ 10^{-6}$	$4.3\ 10^{-6}$	$4.2\ 10^{-6}$	$7.0\ 10^{-6}$	$7.2\ 10^{-6}$
e_x(mm)	1.2	1.2	1.0	3.7	2.0
α_y	0.0	0.4	0.7	-18.6	3.0
β_y(m)	0.23	0.19	0.6	10.2	31.
ϵ_y(m rad)	$6.0\ 10^{-6}$	$7.3\ 10^{-6}$	$1.7\ 10^{-6}$	$1.7\ 10^{-6}$	$0.9\ 10^{-7}$
$\gamma\beta\epsilon_y$(m rad)	$4.0\ 10^{-6}$	$4.7\ 10^{-6}$	$5.0\ 10^{-6}$	$5.0\ 10^{-6}$	$5.4\ 10^{-6}$
e_y(mm)	1.2	1.2	1.0	4.1	1.7
W_0(MeV)	0.100	0.097	1.018	1.018	30.109
$\Delta W/W_0$	0.0	$4.5\ 10^{-2}$	$2.3\ 10^{-2}$	$2.0\ 10^{-2}$	$0.6\ 10^{-3}$
$\Delta\phi°$	17.5	6.5	1.4	0.3	0.3
e_l(mm)	16.0	1.0	0.4	0.5	0.5

REFERENCES

(1) Il Progetto LIS-A dei LNF, LNF July 1987.
(2) F.Tazzioli. Parametri preliminari di un Linac Superconduttore Sperimentale, LNF Memo L-88 Frascati, Feb.1987.
(3) A. Aragona et al. Project of a superconducting RF linac. 3rd workshop on RF superconductivity. Argonne 1987.
(4) U. Amaldi. A superconducting radiofrequency accelerator complex . CERN EP/87-104.
(5) M.Castellano. Caratteristiche del Fascio di Elettroni del Linac Superconduttore per un FEL ad alta efficienza, LNF Memo L-92, May 1987.
(6) Proceedings of the SC Linear Accelerators. Discussion Meeting Frascati Oct.1986.
(7) R.W.Warren et al. The Los Alamos Free Electron Laser: Accelerator Performance. Proc. of the 1984 Free Electron Laser Conf. Castelgandolfo Sept.1984, NIM Vol.A237 (1985) 180-186.
(8) The Continuos Electron Beam Facility (CEBAF).
(9) W.B.Hermannsfeldt SLAC Electron Optics Program. SLAC-166 (1973).
(10) S.Kulinski. Program LISA - to be published.
(11) K.Crandall et al. Program PARMELA - Los Alamos National Laboratory.
(12) S.Kulinski, M.Vescovi. Gun for LISA. Frascati Report LNF-87/98(R).
(13) H. Euteneuer Measurements on $\beta < 1$ segments of the On-Axis-Coupled Structures for the Injector Linac of MAMI. Internal Notiz MAMI 9/84.
(14) H.Euteneuer, H.Scholer. Experiences in Fabrication and testing of the RF-sections of the Mainz Microtron.
(15) M.Preger. Ricircolo per LISA - Internal Memo L-§§.
(16) C.Biscari. Trasporto iniettore-LINAC SC per LISA. Internal memo LIS-2.
(17) B.Bru, M.Weiss. CERN (MPS) Report LIN 74-1.
(18) B.Spataro. Program BEAM. Private comunication.